

Synthesis, characterization and crystal structures of cyclometallated Ru(II) carbonyl complexes formed by hydrazones

Nataraj Chitrapriya^a, Viswanathan Mahalingam^a, Matthias Zeller^b,
Karuppanan Natarajan^{a,*}

^a Department of Chemistry, Bharathiar University, Coimbatore 641 046, India

^b Department of Chemistry, Youngstown State University, Youngstown, OH 44555-3663, USA

Received 7 December 2007; accepted 7 January 2008

Available online 10 March 2008

Abstract

Cyclometallated Ru(II) complexes of the type $[\text{Ru}(\text{CO})(\text{EPh}_3)_2(\text{L})]$ ($\text{E} = \text{P}$ or As ; $\text{L} =$ tridentate hydrazone-derived ligand) have been obtained by refluxing an ethanolic solution of $[\text{RuHCl}(\text{CO})(\text{PPh}_3)_3]$ or $[\text{RuHCl}(\text{CO})(\text{AsPh}_3)_3]$ with the hydrazone derivatives H_2php (2-[(2,4-dinitro-phenyl)-hydrazonomethyl]-phenol), $\text{H}_2\text{p hm}$ (2-[(2,4-dinitro-phenyl)-hydrazonomethyl]-6-methoxy-phenol) and $\text{H}_2\text{p hn}$ (2-[(2,4-dinitro-phenyl)-hydrazonomethyl]-naphthalen-1-ol). The formation of stable cyclometallated complexes has been authenticated by single crystal X-ray structure determination of two of the complexes, and the mechanism of C–H activation is discussed in detail. The spectral (IR, UV–Vis and ^1H NMR) and electrochemical data for all the complexes are reported. Electrochemistry shows a substantial variation in the metal redox potentials with regard to the electronic nature of the substituents present in the hydrazone derivative.
© 2008 Elsevier Ltd. All rights reserved.

Keywords: Ru(II) complexes; Hydrazone-derived ligands; Cyclometallation; Mechanism; Cyclic voltammetry

1. Introduction

The carbon–hydrogen bond is commonly regarded as an unfunctional and unreactive group. Functionalization of C–H bonds remains a problem of great current interest, but many important advances have been made in recent years [1,2]. This has opened up its broad synthetic potential and C–H functionalization has become an important topic in organometallic chemistry [3,4]. Intramolecular C–H activation or cyclometallation reactions are one of the major discoveries of organometallic chemistry that provide access to metallacyclic derivatives of transition metal complexes [5,6], and cyclometallation is one of the most prevalent methods used in activation of C–H bonds in organic molecules [7]. The C–H bond is much stronger than the M–C

bond and the thermodynamic barrier for homolytic cleavage of a C–H bond is high [8]. In general an intramolecular C–H process is favored by both entropy (the chelate effect) and the thermodynamic stability of the resulting cyclic product [9]. The C–H activation obviously depends on both the electron density on the metal and that on the C–H bond that is to be activated, and may be promoted by steric hindrance [10,11]. The interest of chemists in cyclometallated compounds derives from their versatility as well as their numerous applications [12]. These compounds find interesting uses in the fields of organic synthesis [13], the design of new metallomesogenes [14], photochemistry [15], catalysis [16] and liquid crystals [17], and they are used as analytical tools [18] and as antitumor agents [19]. In particular, the functionalization of aromatic rings has attracted much attention [5].

The coordination chemistry of transition metals with ligands from the hydrazine family has been of interest due to different bonding modes shown by these ligands

* Corresponding author. Tel.: +91 422 2424655; fax: +91 422 2422387.
E-mail address: k_nataraj6@yahoo.com (K. Natarajan).

with both electron rich and electron poor metals [20–22]. The mode of bonding depends on the nature of the ligand, the metal ion and the solvent used [23,24]. As the substituents present in the hydrazone strongly influence the reactivity of proximal C–H bonds, a CNO mode of bonding of aryl hydrazones may be expected, provided suitable substituents are located on the aryl ring. With this background, the present work was carried out to study the role of nitro groups towards metal assisted C–H activation of 2,4-dinitrophenyl hydrazone derivatives [25] (Chart 1) using $[\text{RuHCl}(\text{CO})(\text{PPh}_3)_3]$ [26] and $[\text{RuHCl}(\text{CO})(\text{AsPh}_3)_3]$ [27] as the metal complex precursors.

2. Experimental

2.1. Materials and methods

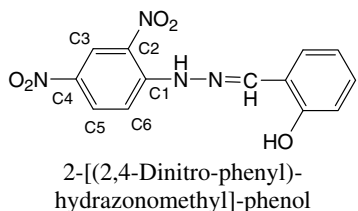
All chemicals were of reagent grade and were used without further purification. Solvents were purified and dried according to standard procedures [25]. Commercially available TBAP (tetra butyl ammonium phosphate) was properly dried and used as a supporting electrolyte for recording cyclic voltammograms of the complexes. FT-IR spectra ($4000\text{--}400\text{ cm}^{-1}$) of the complexes and the free ligand were recorded from KBr pellets with a Nicolet Avatar Model FT-IR spectrophotometer. UV–Vis spectra (800–250 nm) of the complexes were obtained on a Systronics 119 UV–Vis spectrophotometer. ^1H NMR spectra of the complexes were recorded using a Varian-Australia AMX-400 spectrometer. Micro analyses (C, H and N) were performed on a Vario EL III Elementary analyzer. Cyclic voltammograms were recorded on a CHI 1120A electrochemical analyzer with a three electrode compartment consisting of a platinum disc working electrode, platinum wire counter electrode and Ag/Ag^+ reference electrode.

2.2. X-ray crystallography

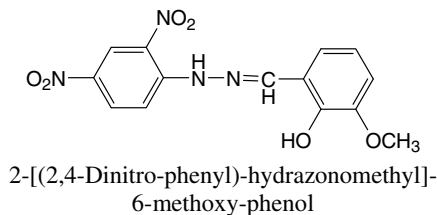
Crystal parameters and details of the collection and refinement are given in Table 1. X-ray diffraction measurements for **1** and **2** were performed on a Bruker AXS SMART APEX CCD diffractometer with graphite mono-

Table 1
Crystal data for **1** and **2**

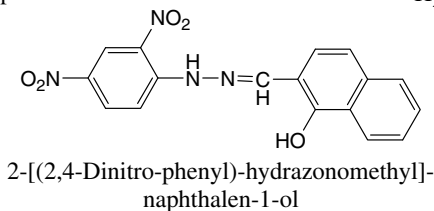
	1	2
Empirical formula	$\text{C}_{53}\text{H}_{45}\text{N}_5\text{O}_7\text{P}_2\text{Ru}_1 \cdot \text{C}_3\text{H}_7\text{NO}$	$\text{C}_{54}\text{H}_{48}\text{N}_5\text{O}_8\text{P}_2\text{Ru}_1$
Formula weight	1026.95	1057.98
Crystal color, habit	red, rod	red, plate
Crystal dimensions (mm)	$0.54 \times 0.25 \times 0.25$	$0.50 \times 0.40 \times 0.10$
Crystal system	monoclinic	monoclinic
Lattice type	primitive	primitive
Space group	$P2_1/n$	$P2/n$
a (Å)	11.7502 (10)	14.0407(8)
b (Å)	26.274 (2)	8.8981(5)
c (Å)	16.1387 (14)	19.0602(11)
α (°)	90	90
β (°)	98.847 (2)	90.2010(10)
γ (°)	90	90
V (Å ³)	4923.1 (7)	2381.3(2)
Z	4	2
Reflections collected	50007	23735
Unique reflections	12232	5909
Reflections $[I > 2\sigma(I)]$	9995	5678
R $[F^2 > 2\sigma(F^2)]$	0.0482	0.0541
wR $[F^2]$	0.1128	0.1251
D_{calc} (Mg m^{-3})	1.386	1.478
F_{000}	2112	1092
μ (Mo $K\alpha$) (mm^{-1})	0.441	0.460
R_{int}	0.0367	0.0313
Goodness-of-fit (S)	1.119	1.225
θ_{max} (°)	30.55	28.28



H_2php



$\text{H}_2\text{p hm}$



$\text{H}_2\text{p hn}$

Chart 1. Structural drawings of the hydrazone derivatives.

chromatized Mo K α radiation. The unit cells were determined using SMART [28] and SAINT+ [29], and the data were corrected for absorption using SADABS [30]. The structures were solved by direct methods and refinements were carried out by full-matrix least-square techniques. The hydrogen atoms were treated by a mixture of independent and constrained refinement. The computer program SHELXTL 6.14 [31] was used for structure solution, refinement and molecular graphics.

The structure of **2** is heavily disordered with both the solvate DMF molecule as well as the complex molecule disordered as a whole. Only the central Ru atom and the phosphine P atom show no disorder. The DMF solvate molecule is disordered around the twofold axis. The two methyl nitrogen distances within the DMF molecule were restrained to be identical within a standard deviation of 0.02 Å, and all DMF atoms were restrained to be isotropic within a standard deviation of 0.1 Å². The different types of disorder within the complex molecule are all related to each other. They are caused by the molecule being located on a crystallographic twofold axis (perpendicular to the Ru–P axis) that is not resembled by the symmetry of the complex molecule. Attempts to solve the structure in the space group Pn (without the twofold axis) resulted in less satisfactory results. The disorder consists in detail of the following. The azo-ligand, which has no twofold symmetry, is rotated by the twofold axis through the Ru atom, resulting in two alternative positions for the ligand with a 1:1 occupancy ratio. The two positions are taking up nearly the same space around the Ru atom. The slight differences for the two orientations are causing disorder for the phenyl rings of the triphenylphosphine ligand, and for the carbon monoxide ligand, which thus also show a 1:1 disorder. For the refinement the following restraints were applied to the complex molecule. All anisotropic displacement parameters of the azo ligand were restraint to have the same U_{ij} components (within a standard deviation of 0.04 for s and 0.08 for st) using a SIMU command in SHELXTL [31]. The carbonyl carbon atoms C51 and C43 and nitrogen atoms N3 and N7 (which are all nearly superimposed with symmetry generated counterparts) were restrained to be isotropic within standard deviations of 0.01 (C51, C43, N7) or 0.001 Å² (N3). All the aromatic rings of the azo ligand and the triphenylphosphine were restrained to be ideal six membered rings (AFIX 66 command) with C–C distances of 1.39 Å. No further positional restraints were applied. All hydrogen atoms were placed in calculated positions and were isotropically refined with a displacement parameter of 1.5 (methyl) or 1.2 times (all others) that of the adjacent carbon atom. With the beta angle in the structure of **2** being very close to 90°, we tested for the possibility of pseudo-merohedral twinning. Refinement using the usual twinning laws (twin instructions 1000–1000–1 and 1000–10001) however, did not result in a significant improvement of the structure quality, and the BASF values refined to values less than one percent. It was thus assumed that the structure was not

twinning and the twin instruction was omitted from the refinement instructions.

2.3. Synthesis

2.3.1. Synthesis of $[Ru(CO)(PPh_3)_2(php)]$ (**1**)

$[RuHCl(CO)(PPh_3)_3]$ (0.1 g, 0.105 mmol) and the ligand H₂php (0.0317 g) were mixed and heated to reflux in dry ethanol (30 mL) for 9 h. The resulting brown crystalline product was collected and washed with cold ethanol and diethyl ether. Subsequent recrystallization by slow diffusion of CHCl₃ vapour into a concentrated DMF solution of the complex yielded brown crystals. Yield: 71 mg (71%). *Anal.* Calc. for C₅₀H₃₈N₄O₆P₂Ru: C, 62.99; H, 4.01; N, 5.87. Found: C, 62.96; H, 4.04; N, 5.84%. IR (KBr) ν/cm^{-1} : 1595 ($\nu C=N$)imine, 1264 ($\nu C-O$). UV/Vis (CHCl₃) λ_{max}/nm ($\epsilon/dm^3 mol^{-1} cm^{-1}$): 264 (11870), 336 (3400), 454 (3820), 504 (3300). ¹H NMR (400 MHz, CDCl₃) δ/ppm : 6.60 (1H, s, CH), 6.90 (1H, s, CH) 7.18–7.85 (multiplet, aromatic protons), 8.4 (1H, s, –CH=N), 11.0 (1H, s, NH).

2.3.2. Synthesis of $[Ru(CO)(PPh_3)_2(phm)]$ (**2**)

This was prepared by the same procedure as **1** with $[RuHCl(CO)(PPh_3)_3]$ (0.1 g, 0.105 mmol) and H₂phm (0.0349 g). Yield: 89 mg (86%). *Anal.* Calc. for C₅₁H₄₀N₄O₇P₂Ru: C, 62.35; H, 4.10; N, 5.70. Found: C, 62.36; H, 4.08; N, 5.74%. IR (KBr) ν/cm^{-1} : 1600 ($\nu C=N$)imine, 1264 ($\nu C-O$). UV/Vis (CHCl₃) λ_{max}/nm ($\epsilon/dm^3 mol^{-1} cm^{-1}$): 263 (21580), 313 (7550), 384 (1710), 515 (345). ¹H NMR (400 MHz, CDCl₃) δ/ppm : 3.90 (3H, s, –OCH₃), 6.47 (1H, s, CH), 6.67 (1H, s, CH) 7.14–7.82 (multiplet, aromatic protons), 8.4 (1H, s, –CH=N), 11.01 (1H, s, NH).

2.3.3. Synthesis of $[Ru(CO)(PPh_3)_2(phn)]$ (**3**)

This was prepared by the same procedure as **1** with $[RuHCl(CO)(PPh_3)_3]$ (0.1 g, 0.105 mmol) and H₂phn (0.0369 g). Yield: 61 mg (58%). *Anal.* Calc. for C₅₄H₄₂N₄O₆P₂Ru: C, 64.50; H, 4.21; N, 5.57. Found: C, 64.56; H, 4.20; N, 5.51%. IR (KBr) ν/cm^{-1} : 1610 ($\nu C=N$)imine, 1254 ($\nu C-O$). UV/Vis (CHCl₃) λ_{max}/nm ($\epsilon/dm^3 mol^{-1} cm^{-1}$): 272 (12650), 359 (5800), 431 (2260). ¹H NMR (400 MHz, CDCl₃) δ/ppm : 6.52 (1H, s, CH), 6.85 (1H, s, CH) 7.12–7.90 (multiplet, aromatic protons), 8.35 (1H, s, –CH=N), 11.0 (1H, s, NH).

2.3.4. Synthesis of $[Ru(CO)(AsPh_3)_2(php)]$ (**4**)

This was prepared by the same procedure as **1** with $[RuHCl(CO)(AsPh_3)_3]$ (0.1 g, 0.107 mmol) and H₂php (0.0323 g). Yield: 77 mg (69%). *Anal.* Calc. for C₅₀H₃₈N₄O₆As₂Ru: C, 57.67; H, 3.67; N, 5.38. Found: C, 57.61; H, 3.68; N, 5.35%. IR (KBr) ν/cm^{-1} : 1607 ($\nu C=N$)imine, 1268 ($\nu C-O$). UV/Vis (CHCl₃) λ_{max}/nm ($\epsilon/dm^3 mol^{-1} cm^{-1}$): 266 (13820), 340 (4450). ¹H NMR (400 MHz, CDCl₃) δ/ppm : 6.58 (1H, s, CH), 6.90 (1H, s, CH) 7.20–7.88 (multiplet, aromatic protons), 8.4 (1H, s, –CH=N), 11.0 (1H, s, NH).

2.3.5. Synthesis of $[Ru(CO)(AsPh_3)_2(phm)]$ (**5**)

This was prepared by the same procedure as **1** with $[RuHCl(CO)(AsPh_3)_3]$ (0.1 g, 0.107 mmol) and H_2phm (0.0356 g). Yield: 87 mg (76%). *Anal. Calc.* for $C_{51}H_{40}N_4O_7As_2Ru$: C, 57.23; H, 3.76; N, 5.23. Found: C, 57.26; H, 3.78; N, 5.27%. IR (KBr) ν/cm^{-1} : 1602 ($\nu C=N$) imine, 1472, 1263 ($\nu C-O$). UV/Vis ($CHCl_3$) λ_{max}/nm ($\epsilon/dm^3 mol^{-1} cm^{-1}$): 268 (3720), 360 (4230). 1H NMR (400 MHz, $CDCl_3$) δ/ppm : 3.90 (3H, s, $-OCH_3$), 6.58 (1H, s, CH), 6.78 (1H, s, CH) 7.0–7.82 (multiplet, aromatic protons), 8.3 (1H, s, $-CH=N$), 11.01 (1H, s, NH).

2.3.6. Synthesis of $[Ru(CO)(AsPh_3)_2(phn)]$ (**6**)

This was prepared by the same procedure as **1** with $[RuHCl(CO)(AsPh_3)_3]$ (0.1 g, 0.107 mmol) and H_2phn (0.0376 g). Yield: 76 mg (65%). *Anal. Calc.* for $C_{54}H_{42}N_4O_6As_2Ru$: C, 59.32; H, 3.87; N, 5.12. Found: C, 59.36; H, 3.88; N, 5.16%. IR (KBr) ν/cm^{-1} : 1610 ($\nu C=N$) imine, 1258 ($\nu C-O$). UV/Vis ($CHCl_3$) λ_{max}/nm ($\epsilon/dm^3 mol^{-1} cm^{-1}$): 268 (24550), 340 (5930), 444 (2560). 1H NMR (400 MHz, $CDCl_3$) δ/ppm : 6.48 (1H, s, CH), 6.75 (1H, s, CH) 7.10–7.86 (multiplet, aromatic protons), 8.38 (1H, s, $-CH=N$), 11.0 (1H, s, NH).

3. Results and discussion

The reaction of 2,4-dinitrophenyl hydrazone ligands with $[RuHCl(CO)(EPh_3)_3]$ ($E = P$ or As) in a 1:1 molar ratio proceeds smoothly in refluxing ethanol, yielding the cycloruthenated complexes through the carbon atom, which is *meta* to both the NO_2 groups, the azomethine nitrogen atom and the phenolate oxygen atom by substitution of one chloride, one of the triphenylphosphines or arsines and one hydride from the Ru(II) precursor. All the complexes are non-hygroscopic, brown in color and found to be air stable at room temperature. Most of the cyclometallation reactions carried out earlier were thought to be favored when the reaction medium contained added bases [32–34] (like NaOH, NaOAc, $N(Et)_3$, etc.), and the presence of electron releasing substituents such as CH_3 , OCH_3 and NH_2 in the aryl ring that is to be cyclometallated seemed to be essential [35,36]. The presence of electron withdrawing substituents such as a NO_2 group on the aryl ring was regarded to inhibit cyclometallation by rendering the aryl ring as an electrophile, which in turn would have made it unavailable for the attack of an electron deficient metal center [37]. In contrast to these two criteria, cyclometallation has been achieved in the present case without any added base in the reaction medium and with the presence of two electron withdrawing NO_2 groups in the hydrazine moiety. A possible explanation could be given the nature of the metal center and that of the electron withdrawing group. The two most likely mechanisms proposed for metal complex promoted C-H activation reactions are oxidative addition and electrophilic substitution. These two alternatives have different requirements for electron density at the metal center. The metal center may behave

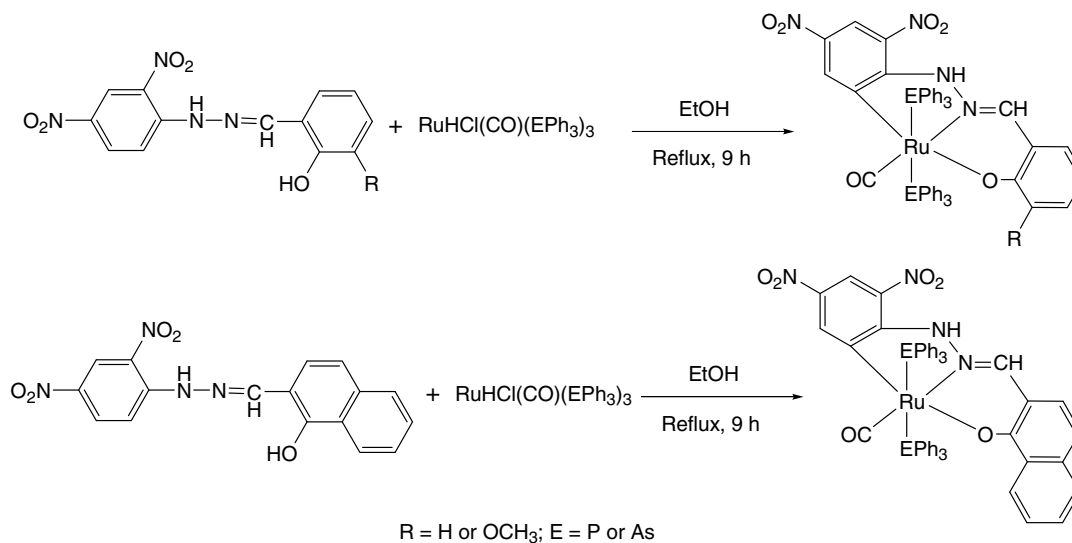
as an electrophile or as a nucleophile in its attack on the aromatic ring. In general, electrophilic attack is favored by electron poor metal centers whilst oxidative addition is favored by electron rich metal centers. There are many instances of cyclometallation where the oxidative addition and electrophilic mechanism cannot be easily distinguished [38,39]. In the present case the C–H activation seems to proceed via an electrophilic attack of the electron deficient metal center on the C–H bond present in the aryl ring which is *meta* to both the nitro substituents. The primary ligands (CO and $PPh_3/AsPh_3$) present in the precursor complexes are π -acidic in nature and are capable of acquiring electron density from the metal through back bonding, thereby making the metal center electron deficient (an electrophile). At the same time, the *meta*-directing NO_2 groups, which are *meta* to each other, withdraw electron density only from the C3 (*ortho* to both NO_2 groups) and C5 (*ortho* to the 4- NO_2 group and *para* to the 2- NO_2 group) atoms and makes the C6 atom (*meta* to both NO_2 groups) relatively electron rich (a nucleophile). These two key steps, i.e. the formation of an electrophile and a nucleophile initiate cyclometallation, which is propagated through a series of steps as detailed below Scheme 1.

3.1. Mechanism for C–H activation

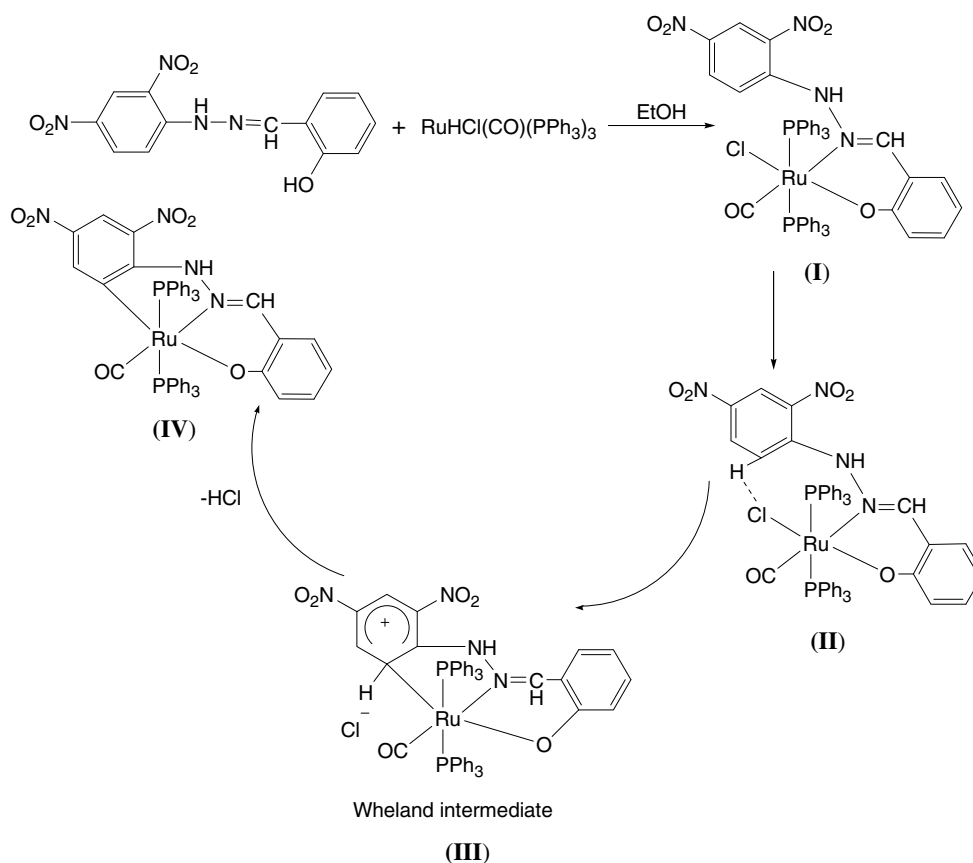
On the basis of the above points, the mechanism of the C–H activation has been deduced and depicted in Scheme 2. In the first step, the weakly coordinated hydrido ligand and a neutrally coordinated $PPh_3/AsPh_3$ are substituted by the phenolate oxygen and azomethine nitrogen of the hydrazone ligand. In the second step, the metal center is located in close proximity to the C6 atom of the aryl ring to be cyclometallated, which has become a nucleophile due to the *meta*-directing effect of the NO_2 groups. Then, the C6–H bond is considerably weakened by the interaction of the proton with the metal bound chloride and may be envisaged as an activated bond. In the next step, the electrophilicity of the ruthenium center is further increased due to the reduced σ -donation of the chloride to the metal center. The electrophilic attack at the C6–H bond is instigated by **II** affording the Wheland intermediate **III** and deprotonation occurs subsequently to expel HCl. The proposed electrophilic substitution is supported by the elimination of HCl during the cyclometallation, which is a unique feature of the electrophilic pathway [5,40,41].

3.2. IR spectra

The important IR frequencies of the complexes are given in the experimental section. The band due to NH stretching in the free ligands occurs in the 3400–3290 cm^{-1} region and remains unaffected after complexation. This precludes the possibility of coordination through the hydrazinic nitrogen atom. In the IR spectra of the complexes a considerable negative shift in $\nu(C=N)$ is observed, indicating coordina-



Scheme 1. Synthesis of complexes 1–6.



Scheme 2. Proposed mechanism for C–H activation.

tion through the azomethine nitrogen atom. The hypsochromic shift of the N–N vibration also supports the above coordination. A peak at around 3100 cm⁻¹ due to $\nu(\text{O–H})$ stretching is absent in the spectra of the complexes, suggesting the deprotonation of the –OH group of the ligands prior to coordination to the metal. The $\nu(\text{C–O})$ phenolic modes of the ligands appearing in the region 1218–

1222 cm⁻¹ are shifted to 1254–1268 cm⁻¹ in the complexes, indicating complex formation via deprotonation of the phenolic OH. The presence of the nitro group in the complexes are characterized by the two bands observed at around 1518–1534 cm⁻¹ and 1322–1340 cm⁻¹ which arise due to symmetric and asymmetric stretching modes of NO₂.

3.3. Electronic spectra

The UV–Vis spectral bands of all the complexes were measured in dichloromethane. All the complexes exhibited two to four bands in the region 264–504 nm. The two absorption bands appearing in the range 264–272 nm and 336–360 nm may be assigned to a $\pi \rightarrow \pi^*$ transition of the aromatic ring and a $n \rightarrow \pi^*$ transition of the $-\text{C}=\text{N}$ group, respectively. In addition, the low energy absorption peaks in the wavelength range 431–504 nm are associated with a charge transfer transition. The spectra of the complexes do not show any d–d transitions [42,43].

3.4. ^1H NMR spectra

^1H NMR spectra of the complexes show all the expected signals. In all the spectra, a singlet corresponding to a single proton is observed in the range δ 8.0–8.4 ppm, which is attributed to the azomethine proton ($-\text{HC}=\text{N}$). The singlet due to the NH proton appears at δ 11.0 ppm. Two singlets observed around δ 6.40–6.60 and 6.70–6.90 ppm are due to the protons of the metallated ring. The triphenylphosphine/triphenylarsine and other ring protons are observed as overlapping signals around δ 7.1–7.9 ppm. A sharp singlet at δ 3.9 ppm is assigned to the methoxy protons of complexes **2** and **5**.

3.5. X-ray crystallography

The molecular structures of complexes **1** and **2** have been determined by single crystal X-ray diffraction. The molecular structures of **1** and **2** are shown in Figs. 1 and 2. Selected bond distances and bond angles are given in Table 2. The RuNOC_2P_2 coordination sphere is distorted octahedral, as can be seen from the angles subtended at the ruthenium center. The basal plane is made up from C, N and O atoms of the dibasic tridentate hydrazone ligand and one carbonyl carbon, while the two PPh_3 groups occupy the apical positions. The structure shows that the hydrazone ligand is coordinated to Ru through the imine

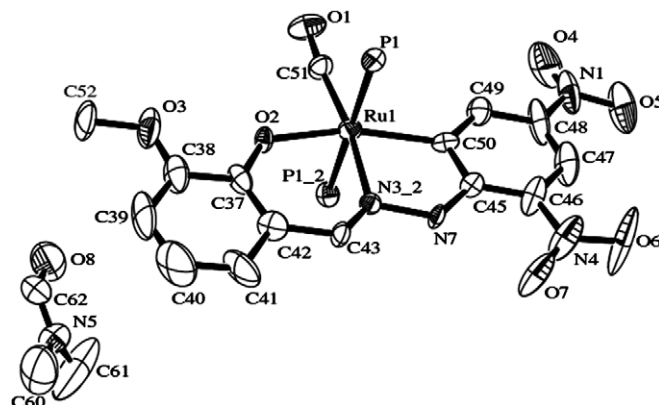


Fig. 2. Labelled ORTEP diagram of **2** with the thermal ellipsoids at 50% probability. Hydrogen atoms and phenyl rings of PPh_3 are omitted for clarity.

nitrogen, phenolic oxygen and aryl carbon, forming a six membered ring by O, N chelation and a five member ring by C, N chelation with bite angles $\text{O5}-\text{Ru1}-\text{N4}$ (87.75°) and $\text{N4}-\text{Ru1}-\text{C37}$ (80.15°). From the covalent radii values, the $\text{Ru(II)}-\text{C}(\text{sp}^2)$ length is estimated to be 2.06 \AA [44] and the observed values span the range $1.96\text{--}2.16 \text{ \AA}$ [45]. In our complex the $\text{Ru1}-\text{C37}$ distance is 2.040 \AA , which is identical to that of the other structurally characterized cyclometallated Ru(II) complexes [46,33]. The $\text{Ru1}-\text{C50}$ bond distance (1.860 \AA) is in accordance with those found in another Ru(II) complex [47]. The $\text{Ru}-\text{C37}(\text{sp}^2)$ bond is 0.18 \AA longer than the $\text{Ru1}-\text{C50}(\text{sp})$ distance, due to $\text{Ru}-\text{CO}$ back bonding. The two $\text{Ru}-\text{P}$ bond lengths are similar and are comparable to those reported for other PPh_3 coordinated Ru(II) complexes [48,49]. The $\text{Ru1}-\text{O5}(\text{phenolato})$ distance of 2.139 \AA is slightly longer than those reported previously for similar Ru(II) complexes [50–53]. This lengthening of the $\text{Ru}-\text{O}$ bond distance can be explained by the trans influence of the soft aryl carbon atom which is present trans to the phenolic oxygen. The trans weakening effect of CO is evident in the $\text{Ru1}-\text{N4}$ bond distance (2.065 \AA), which is significantly longer than those that found for $[\text{Ru}(\text{pabh})_2]$ [54] ($\text{pabh} = N\text{-(aryl)-}N'$ -(picolinylidene)hydrazine) ($1.960(3)$ and $1.958(3) \text{ \AA}$), $\text{trans-}[\text{Ru}(\text{pamh})(\text{PPh}_3)_2\text{Cl}]$ [55] ($\text{pamh} = N\text{-(aryl)-}N'$ -(picolinylidene)hydrazine) ($1.933(3) \text{ \AA}$), $[\text{Ru}(\text{HL})(\text{PPh}_3)\text{Cl}]\text{Cl}$ ($1.984(5) \text{ \AA}$) and $[\text{Ru}(\text{HL})(\text{PPh}_3)(\text{mpi})\text{Cl}]_2$ ($1.991(5) \text{ \AA}$) ($\text{HL} = \text{methyl 2-pyridylketone 4-(4-tolyl)thiosemicarbazones}$), ($\text{mpi} = \text{methyl (2-pyridyl)methyleneimine}$)) [56].

3.6. Electrochemistry

Dichloromethane solutions of the complexes have been used to study the electrochemical properties, with the help of cyclic voltammetry. The potential data are listed in Table 3 and a representative voltammogram of **2** is illustrated in Fig. 3. The potentials of both the metal centered oxidation and reduction reflect the influence of the electronic nature of the substitutions present in the ligands.

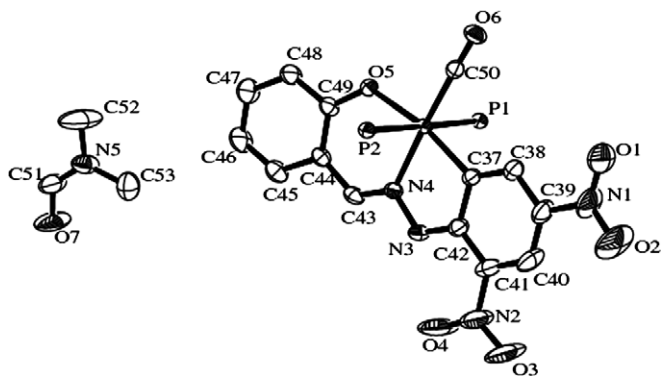


Fig. 1. Labelled ORTEP diagram of **1** with the thermal ellipsoids at 50% probability. Hydrogen atoms and phenyl rings of PPh_3 are omitted for clarity.

Table 2
Selected bond lengths (Å) and bond angles (°) for **1** and **2**

1		2	
Ru1–C50	1.860(3)	Ru1–C51	1.840(5)
Ru1–C37	2.040(3)	Ru1–C50	2.202(4)
Ru1–N4	2.065(2)	Ru1–N3	2.065(3)
Ru1–O5	2.1391(18)	Ru1–O2	2.023(5)
Ru1–P1	2.3792(7)	Ru1–P1	2.3914(7)
Ru1–P2	2.3837(7)	Ru1–P2	2.3914(7)
C50–Ru1–C37	95.99(11)	C51–Ru1–C50	95.2(2)
C50–Ru1–N4	176.08(10)	C51–Ru1–N3	170.9(4)
C50–Ru1–O5	96.11(9)	C51–Ru1–O2	100.7(3)
C50–Ru1–P1	88.59(8)	C51–Ru1–P1	92.4(4)
C50–Ru1–P2	89.93(8)	C51–Ru1–P2	87.5(4)
C37–Ru1–N4	80.16(10)	C50–Ru1–N3	78.1(4)
C37–Ru1–O5	167.88(9)	C50–Ru1–O2	163.8(2)
C37–Ru1–P1	89.82(7)	C50–Ru1–P1	90.98(18)
C37–Ru1–P2	90.21(7)	C50–Ru1–P2	89.1(7)
N4–Ru1–O5	87.75(8)	N3–Ru1–O2	85.8(4)
N4–Ru1–P1	92.11(6)	N3–Ru1–P1	87.8(4)
N4–Ru1–P2	89.36(6)	N3–Ru1–P2	92.4(4)
O5–Ru1–P1	89.90(5)	O2–Ru1–P1	91.28(18)
O5–Ru1–P2	90.39(5)	O2–Ru1–P2	88.73(18)
P1–Ru1–P2	178.51(2)	P1–Ru–P2	179.81(4)

Hydrogen bonding geometry for **2**

D–H···A	D–H (Å)	H···A (Å)	D···A (Å)	D–H–A (°)
N7–H7A···O1	0.88	2.61	3.395(10)	149(5)
N7–H7A···O7	0.88	1.93	2.563(11)	127(8)

Table 3
Cyclic voltammetric data for the Ru(II) complexes

Complex	Ru(III)/Ru(II) ^a $E_{1/2}$ / V(ΔE_p /mV)	Ru(II)/Ru(I) ^b $E_{1/2}$ / V(ΔE_p /mV)	Ligand based reduction ^d
1	0.84 ^c	–0.42(210)	–1.28
2	0.92 (1080)	–0.55(460)	–1.18
3	0.82 ^c	–0.40(250)	–1.30
4	0.83 ^c	–0.50(400)	–1.24
5	0.84 ^c	–0.60(520)	–1.28
6	0.83 ^c	–0.48(680)	–1.34

^a Oxidation couple.

^b Reduction couple.

^c Irreversible, E_{p_a} value.

^d Irreversible, E_{p_c} value.

Each complex displays a reductive response on the negative side and an oxidative response on the positive side of the Ag/AgCl electrode. The oxidation couple observed for complex **2** is assigned to the Ru(III)–Ru(II) oxidation. In all the other complexes, the Ru(III)–Ru(II) oxidation process takes place irreversibly in the range 0.82–0.84 V. Thus, as the σ -bonding ability of the O-atom of the deprotonated phenol functionality decreases with the increasing electron withdrawing ability of the substituents, the Ru(III)–Ru(II) oxidation becomes more difficult. The reductive response, observed in the range –0.40 to –0.60 V is quasireversible with a peak-to-peak separation (ΔE_p) of 210–680 mV, and it is attributed to the Ru(II)–Ru(I) couple. The electron withdrawing substituents on the ligands have a significant effect on the observed reduction peak potentials. Electron withdrawing groups lower the electron density on the metal center even further and lead to less negative

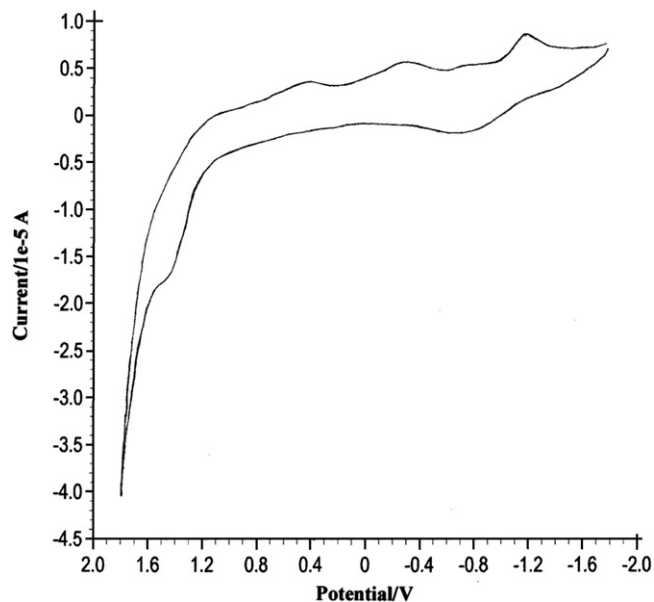


Fig. 3. Cyclic voltammogram of complex **2**.

potentials than for complexes with electro releasing groups. In addition, the M–C bond largely lowers the redox potentials of Ru(II) complexes [3]. Generally, the presence of an electron withdrawing group stabilizes the lower oxidation state and an electron donating group favors the higher oxidation state of the metal. The cyclic voltammograms of all the complexes were unailing with one irreversible ligand based reduction due to the reduction of the HC=N group. These reduction peaks were shifted to more negative potentials with respect to the free ligands, which was consistent with the complex formation. It is interesting to note that a substituent which is somewhat away from the electroactive metal center can influence the metal centered redox potentials in a predictable manner.

4. Conclusion

A new family of cyclometallated Ru(II) complexes has been prepared and characterized. This C–H activation process is believed to proceed via an electrophilic substitution mechanism. What is more interesting is that the cyclometallation reaction presented here takes place under neutral conditions and without auxiliaries. Voltammetric results obtained in this study showed that the hydrazone ligands stabilize a lower oxidation state of the metal complexes. The substituents on the hydrazone ligands were found to have a significant effect on the redox potential. All the new complexes seem of interest for general synthetic and theoretical chemical research and may have some potential for catalytic applications.

Appendix A. Supplementary data

CCDC 663252 and 613459 contain the supplementary crystallographic data for **1** and **2**. These data can be

obtained free of charge via <http://www.ccdc.cam.ac.uk/conts/retrieving.html>, or from the Cambridge Crystallographic Data Centre, 12 Union Road, Cambridge CB2 1EZ, UK; fax: (+44) 1223-336-033; or e-mail: deposit@ccdc.cam.ac.uk. Supplementary data associated with this article can be found, in the online version, at [doi:10.1016/j.poly.2008.01.032](https://doi.org/10.1016/j.poly.2008.01.032).

References

- [1] Y. Guari, S. Sabo-Etienne, B. Chaudret, *Eur. J. Inorg. Chem.* (1999) 1047.
- [2] S. Niu, M.B. Hall, *J. Am. Chem. Soc.* 120 (1998) 6169.
- [3] A.D. Ryabov, V.S. Sukharev, L. Alexandrova, R.L. Lagadec, M. Pfeffer, *Inorg. Chem.* 40 (2001) 6529.
- [4] T. Matsubara, N. Koga, D.G. Musaev, K. Morokuma, *J. Am. Chem. Soc.* 120 (1998) 12692.
- [5] A.E. Shilov, G.B. Shulpin, *Chem. Rev.* 97 (1997) 2879.
- [6] D.J. de Geest, B.J. O'keefe, P.J. Stell, *J. Organomet. Chem.* 97 (1999) 579.
- [7] V. Ritling, C. Sirlin, M. Pfeffer, *Chem. Rev.* 102 (2002) 1713.
- [8] J. Halpern, *Acc. Chem. Res.* 15 (1982) 238.
- [9] I.C.M. Wehman-Ooyevaar, I.F. Luitwieler, K. Vatter, D.M. Grove, W.J.J. Smeets, E. Horn, A.L. Spek, G. van Koten, *Inorg. Chim. Acta* 252 (1996) 55.
- [10] H.L.L. Abbenhuis, M. Pfeffer, J.-P. Sutter, A. de Cian, J. Fischer, *Organometallics* 12 (1993) 4464.
- [11] P.L. Alsters, P.F. Engel, M.P. Hogerheide, M. Copijn, A.L. Spek, G. van Koten, *Organometallics* 12 (1993) 1831.
- [12] C. Cativaela, L.R. Falvello, J.C. Gines, R. Navarro, E.P. Urriolabeitia, *New J. Chem.* 25 (2001) 344.
- [13] G. Zhao, Q.G. Wang, T.C.W. Mak, *J. Organomet. Chem.* 311 (1999) 574.
- [14] P. Espinet, M.A. Esteruelas, L.A. Oro, J.L. Serrano, E. Sola, *Coord. Chem. Rev.* 17 (1992) 215.
- [15] A. Von zelewsky, P. Belser, P. Hayoz, R. Dux, X. Hua, A. Suckling, H. Stoeckli-Evans, *Coord. Chem. Rev.* 75 (1994) 132.
- [16] J. Dupont, M. Pfeffer, J. Spencer, *Eur. J. Inorg. Chem.* (2001) 1917.
- [17] D.J. Saccomando, C. Black, G.W.V. Cave, D.P. Lydon, J.R. Rourke, *J. Organomet. Chem.* 305 (2001) 601.
- [18] E.P. Urriolabeitia, M.D. Diaz-de-villegas, *J. Chem. Edu.* 77 (1999) 76.
- [19] J.D. Higgins, *J. Inorg. Biochem.* 49 (1993) 149.
- [20] M. Wang, E.W. Volkert, P.R. Singh, K.K. Katti, P. Lusiak, K.V. Katti, C.L. Barnes, *Inorg. Chem.* 33 (1994) 1184.
- [21] K.V. Katti, V.S. Reddy, P.R. Singh, *Chem. Soc. Rev.* 24 (1995) 97.
- [22] K.V. Katti, P.R. Singh, C.L. Barnes, *Inorg. Chem.* 31 (1992) 4588.
- [23] R.M. Issa, H. El-Baradie, M. Gaber, *Egypt J. Chem.* 31 (1988) 251.
- [24] M.F. Iskander, L. El-Sayed, N.M. Salem, R. Werner, W. Haase, *J. Coord. Chem.* 56 (2003) 1075.
- [25] A.I. Vogel, *Text Book of Practical Organic Chemistry*, 5th ed., Longman, London, 1989.
- [26] N. Ahmed, J.J. Lewison, S.D. Robinson, M.F. Uttley, *Inorg. Synth.* 15 (1974) 48.
- [27] R.A.S. Pelgado, W.Y. Lee, S.R. Choi, Y. Cho, M.J. Jun, *Trans. Met. Chem.* 16 (1991) 241.
- [28] Bruker Advanced X-ray Solutions SMART for WNT/2000 (Version 5.628), Bruker AXS Inc., Madison, WI, USA, 1997–2002.
- [29] Bruker Advanced X-ray Solutions SAINT (Version 6.45), Bruker AXS Inc., Madison, WI, USA, 1997–2003.
- [30] Bruker Advanced X-ray Solutions SADABS in SAINT (Version 6.45), Bruker AXS Inc., Madison, Wisconsin, USA, 1997–2003.
- [31] G.M. Sheldrick, SHELXTL v.6.14, Bruker AXS Inc., Madison, WI, 2003.
- [32] S. Fernandez, M. Pfeffer, V. Ritleng, C. Sirlin, *Organometallics* 18 (1999) 2390.
- [33] V. Perez, A. Riera, A. Rodriguez, D. Miguel, *Organometallics* 21 (2002) 5437.
- [34] D.L. Davies, O. Al-Duaij, J. Fawcett, M. Giardiello, S.T. Hilton, D.R. Russell, *J. Chem. Soc., Dalton Trans.* (2003) 4132.
- [35] H. Takahashi, J. Tsuji, *J. Organomet. Chem.* 10 (1967) 511.
- [36] J. Vicente, I. Saura-Llamas, P.G. Jones, *J. Chem. Soc., Dalton Trans.* (1993) 3619.
- [37] A.C. Cope, E.C. Friedrich, *J. Am. Chem. Soc.* 90 (1968) 909.
- [38] R.L. Brainard, W.R. Nutt, T.R. Lee, G.M. Whitesides, *Organometallics* 7 (1988) 2379.
- [39] R. Cordone, W.D. Harman, H. Taube, *J. Am. Chem. Soc.* 111 (1989) 2896.
- [40] G.B. Shulpin, G.V. Nizova, A.T. Nikitaev, *J. Organomet. Chem.* 276 (1984) 115.
- [41] C. Crocker, R.J. Errington, R. Markham, C.J. Moulton, B.L. Shaw, *J. Chem. Soc., Dalton Trans.* (1982) 387.
- [42] A.R. Salib, S.L. Stefun, S.M.A. El-Wafa, H.F. El-Shafiy, *Synth. React. Inorg. Met.-Org. Chem.* 31 (5) (2001) 895.
- [43] M.A. Greaney, C.L. Coyle, M.A. Harmer, A. Jordan, E.I. Stifel, *Inorg. Chem.* 28 (1989) 912.
- [44] A.K. Rappe, C.J. Casewit, K.S. Colwell, W.A. Goddard, W.M. Skiff, *J. Am. Chem. Soc.* 114 (1992) 10024.
- [45] M.D. Fryzuk, C.D. Montgomery, S.J. Rettig, *Organometallics* 10 (1991) 467.
- [46] H. Aneetha, C.R.K. Rao, K.M. Rao, P.S. Zacharias, X. Feng, T.C.W. Mak, B. Srinivas, M.Y. Chiang, *J. Chem. Soc., Dalton Trans.* (1997) 1697.
- [47] A. Hijazi, J.-P. Djukic, M. Pfeffer, L. Ricard, N.K. Gruber, J. Raya, P. Bertani, A. deCian, *Inorg. Chem. Commun.* 45 (2006) 4586.
- [48] K. Nareshkumar, R. Ramesh, Yu Liu, *J. Inorg. Biochem.* 100 (2006) 18.
- [49] P. Ghosh, A. Pramanik, A. Chakravorty, *Organometallics* 15 (1996) 4147.
- [50] S. Chakraborty, M.G. Walawalkar, G.K. Lahiri, *J. Chem. Soc., Dalton Trans.* (2000) 2875.
- [51] V.R.L. Constantino, H.E. Toma, L.F.C. de Oliveira, F.N. Rein, R.C. Rocha, D.O. Silva, *J. Chem. Soc., Dalton Trans.* (1999) 1735.
- [52] P. Bhattacharyya, M.L. Loza, J. Parr, A.M.Z. Slawin, *J. Chem. Soc., Dalton Trans.* (1999) 2917.
- [53] S.A. Serron, C.M. Haar, S.P. Nolan, *Organometallics* 16 (1997) 5120.
- [54] S. Pal, S. Pal, *J. Chem. Soc., Dalton Trans.* (2002) 2102.
- [55] R. Raveendran, S. Pal, *Polyhedron* 24 (2005) 57.
- [56] M. Maji, M. Chatterjee, S. Ghosh, S.K. Chattopadhyay, B.-M. Wu, T.C.W. Mak, *J. Chem. Soc., Dalton Trans.* (1999) 135.